Vertical-axis wind turbine analysis using blockage-tolerant wind tunnel results for post-stall aerofoils

John Rainbird, Joaquim Peiro, Mike Graham
Department of Aeronautical Engineering, Imperial College, London, UK

1 Introduction

VAWT performance is sensitive to small changes in aerofoil characteristics at certain post-stall angles [6], particularly during start-up when the blades experience a wide range of angles of incidence. Accurate post-stall data is therefore desirable for the study of these machines. To demonstrate the sensitivity of VAWTs to post-stall aerofoil performance, two simulations of start-up have been performed using a blade-element momentum, BEM, model (Strickland's multiple-streamtube method [13]) and are shown in Fig. 1.

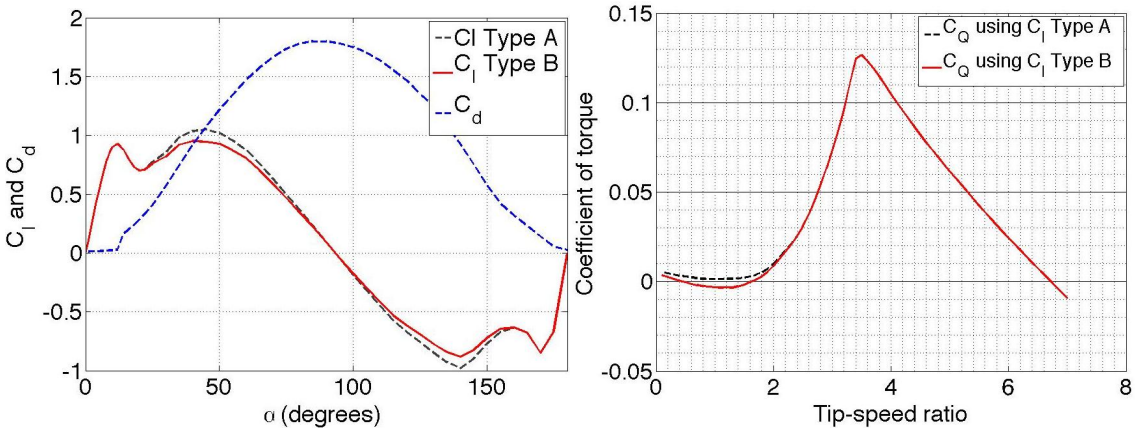

(a) Aerofoil coefficients [12]

(b) Turbine C_p envelope

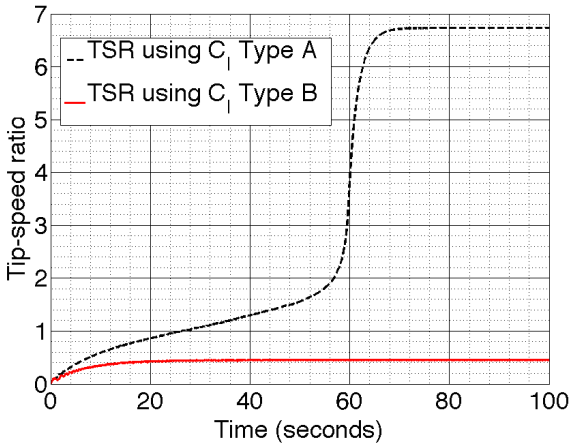

(c) Turbine start-up behaviour

Figure 1: Effects of small changes in post-stall lift on VAWT performance.

Simulation Type A uses blade characteristics taken from Sheldahl and Klimas's post-stall study [12], while Type B has a lift characteristic modified to exhibit 10% lower post-stall peaks in C_l

at incidences of $45°$ and $135°$, see Fig. 1a. This small change in input blade data is sufficient to significantly impact on the predicted development of tip-speed ratio, TSR, with time from a standing start, as shown in Fig. 1c. Turbine A accelerates along the whole of its torque curve to the highest equilibrium state at a TSR of 6.7. Type B shares the same highest equilibrium state, but accelerates only as far as an earlier equilibrium state at TSR = 0.4, beyond which at $0.4 <$TSR< 1.6 negative torques are induced, see Fig. 1b.

Little post-stall aerofoil data exists covering a full range of incidences from $0°$ to $180°$, there is a particular lack of data taken at the low Reynolds numbers at which small-to-mid-scale VAWT blades operate. Fig. 2 reproduces C_l and C_d from the studies of Bergeles et al. [1], Critzos et al. [3], Massini et al. [7] and Sheldahl and Klimas [12] for the NACA 0012 and Pope's study [9] of the NACA 0015, results for which should be similar to the NACA 0012, particularly post-stall.

There is excellent agreement with thin aerofoil theory for all studies pre-stall but post-stall the spread of data is far wider. At the second lift peak at $\alpha \approx 45°$, values of C_l vary between 0.98 and 1.18, a difference of 20%. At peak drag at $\alpha \approx 90°$, C_d is between 1.81 and 2.08, a 15% variation. The variation in the lift peak is more than sufficient to impact on accurate modelling of VAWT start-up, suggesting more accurate post-stall data is required to simulate start-up with confidence. These uncertainties in aerofoil characteristics are perhaps the reason that, in spite of experimental studies showing that VAWTs with straight, symmetrical blades are capable of self-starting [4, 6, 10], accurate modelling of successful start-up can prove difficult without modification of the input aerofoil coefficient data. For instance, Bianchini et al. give their blades "virtual camber" [2] while Rossetti and Pavesi [11] apply the post-stall model of Viterna and Corrigan [14] to their blades.

Where studies have varied Reynolds number, the impact of this on post-stall performance has been far less significant than the differences seen in Fig. 2 [3, 12]. The differences are therefore the result of discrepancies between experiments, the most likely being the extent to which wind tunnel blockage has affected readings, and the steps taken to minimise this.

Solid wind tunnel walls constrain streamline curvature induced by a test model and models and walls together block the flow through the tunnel, causing it to speed up around the model. Blockage corrections are used to reduce these effects. Derived using potential flow theory for streamline constraints and using potential flow and empirical methods for blockage, these corrections are applicable only to attached flows, though with caution they can be applied to flows with "some degree of separation" [5]. Their use with deeply stalled aerofoils, where flow is fully separated, is therefore questionable and could be responsible for the poor agreement between the existing post-stall data.

Pope's study used a "breather" in his wind tunnel to limit blockage and applied corrections for streamline curvature [9]. All other referenced studies used conventional solid walled tunnels and applied corrections for streamline curvature and blockage.

2 Approach

Blockage tolerant test sections offer a means of minimising blockage effects without the need for corrections. Since corrections for closed and open jets are of opposite signs [5], one would expect that free air conditions can be approximated using semi-permeable walls. Parkinson's design [8] has been used in this study, see Fig. 3 for a diagram. Slotted walls comprised of a regular array of evenly spaced aerofoils perpendicular to the flow allow flow to exit and re-enter the main channel, the shape of the array components avoiding flow separation around them. The slatted wall regions are enclosed by plenum chambers to maintain mass conservation in the flow along the tunnel.

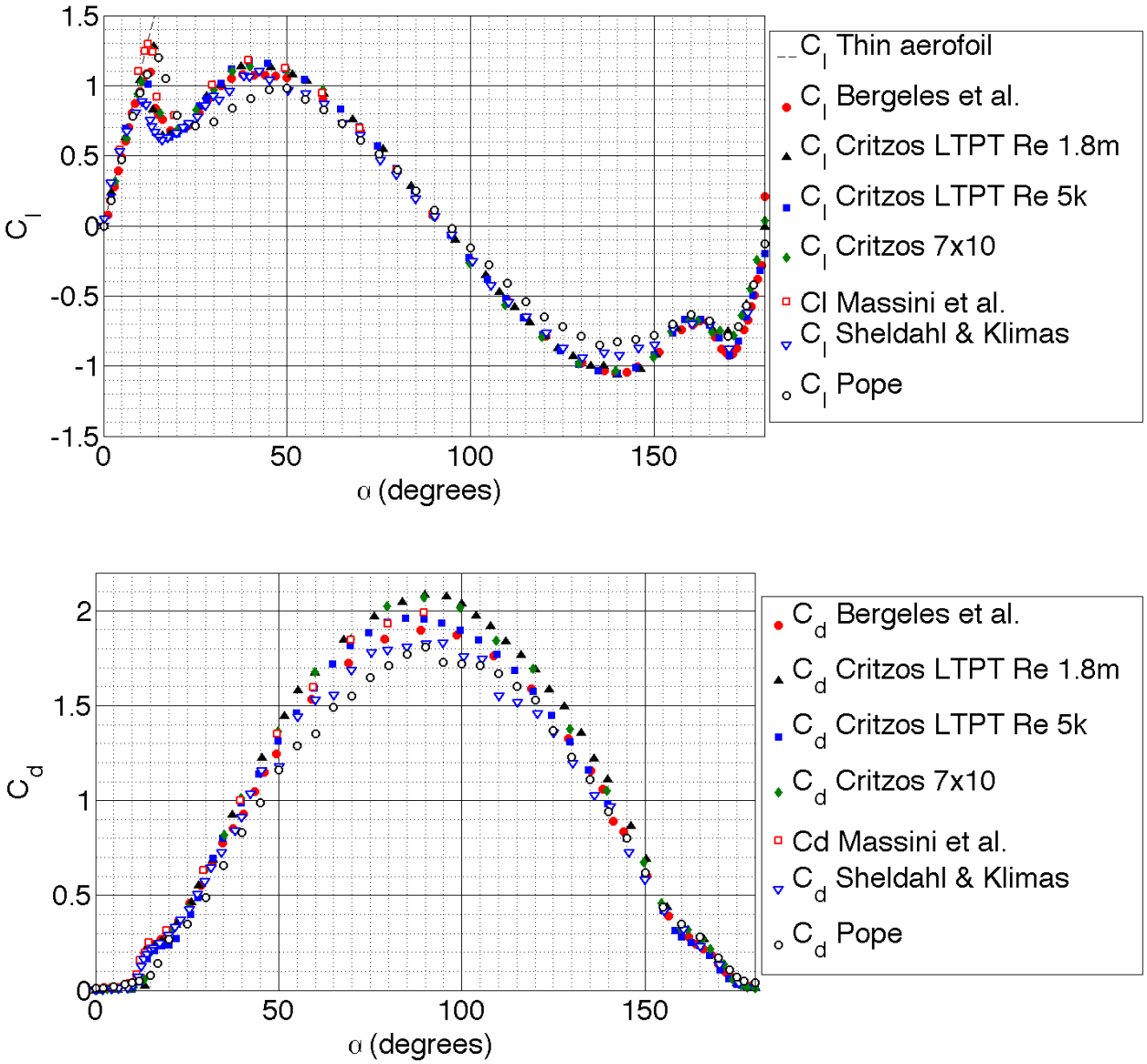

Figure 2: C_l and C_d vs α for the $c/H = 0.32$ aerofoil from this study, alongside the studies of Bergeles et al [1], Critzos et al. [3], Massini et al [7], Sheldahl and Klimas [12] and Pope [9].

An appropriate open area ratio (OAR, a ratio of open to slatted wall areas, defined as g/s in Fig. 3) must be obtained through experiments on models of different sizes but with like shapes, maintaining a constant Reynolds number throughout. The OAR that gives the most similar results for the models is that which provides the closest approximation of unconstrained steady flow, since in free air results would be identical regardless of model size.

Fig. 4 shows a cutaway view of the Imperial College facility built to Parkinson's design. The aerofoil under test is mounted vertically between endplates which sit flush with the tunnel walls. Force transducers are mounted at both ends of the aerofoil to measure aerodynamic forces and moments, with the upper one mounted to a bearing unit that allows free rotation. The lower one is attached to a stepper motor to control incidence. The slatted walls can be replaced with solid walls

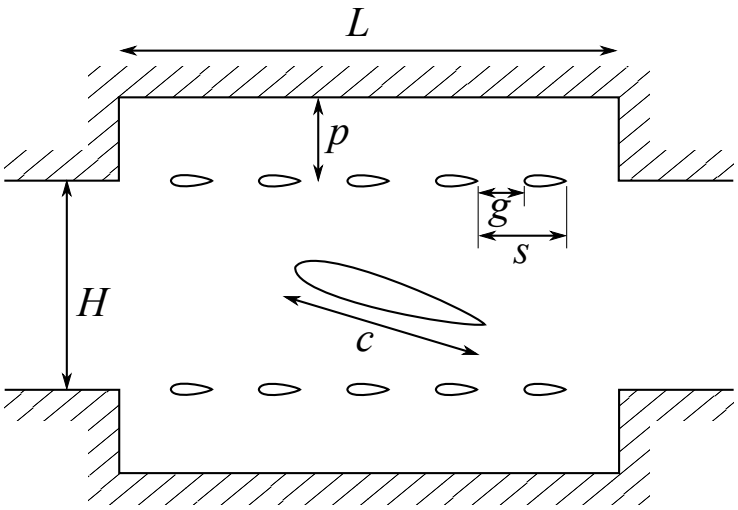

Figure 3: Parkinson's slatted-walled tolerant tunnel.

to replicate a conventional test section, or one wall can be left slatted for an asymmetric tolerant tunnel.

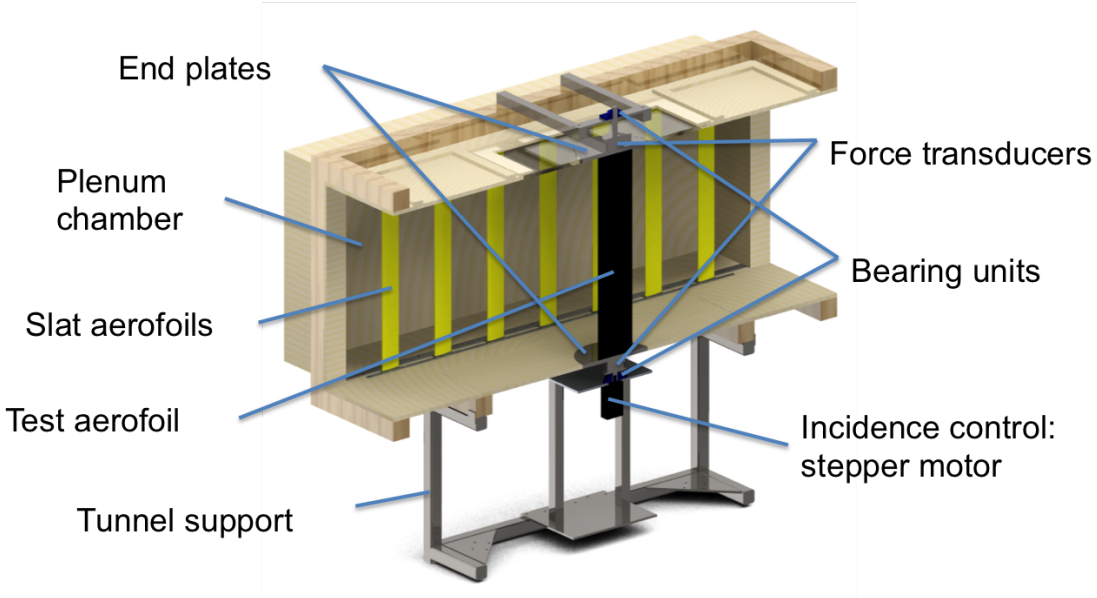

Figure 4: Streamwise cutaway view of the Imperial College Parkinson tunnel.

3 Main Body

Tests have been conducted on five NACA 0015 aerofoils with chord-to-tunnel height ratios, c/H, of 0.1, 0.15, 0.2 0.25 and 0.3. The larger the aerofoil in comparison to the wind tunnel, the more it will be affected by blockage. Various configurations of the tolerant wind tunnel were tried, with single slatted walls or two slatted walls, at a range of OARs. Reynolds numbers of 60000, 150000 and

250000 were used. The conventional, solid walled set up was also used to judge how well current best practice performs in terms of similarity of results for the five aerofoils.

The performance of the tunnels was judged by taking a standard deviation (SD) of results for the five aerofoils at each incidence at which readings were taken. For the solid walled tunnel, blockage corrections were applied to data before taking the SDs. These were then summed across the range of incidences tested, separated into pre-stall ($-2°$ to $10°$) and post stall ($-20°$ to $160°$) regions, for lift and drag. The lower the sum of SDs, the better the tunnel has performed since the results for the five aerofoils are closer.

Fig. 5 shows the results of the SD analysis for double and single slatted wall tunnels at $Re = 150000$. It can be seen that the 71% OAR double slatted wall tunnel performs best of all the tolerant configurations, with the lowest SD summations either side of stall for lift and drag. It also performs better than the corrected conventional tunnel for all other than post-stall drag.

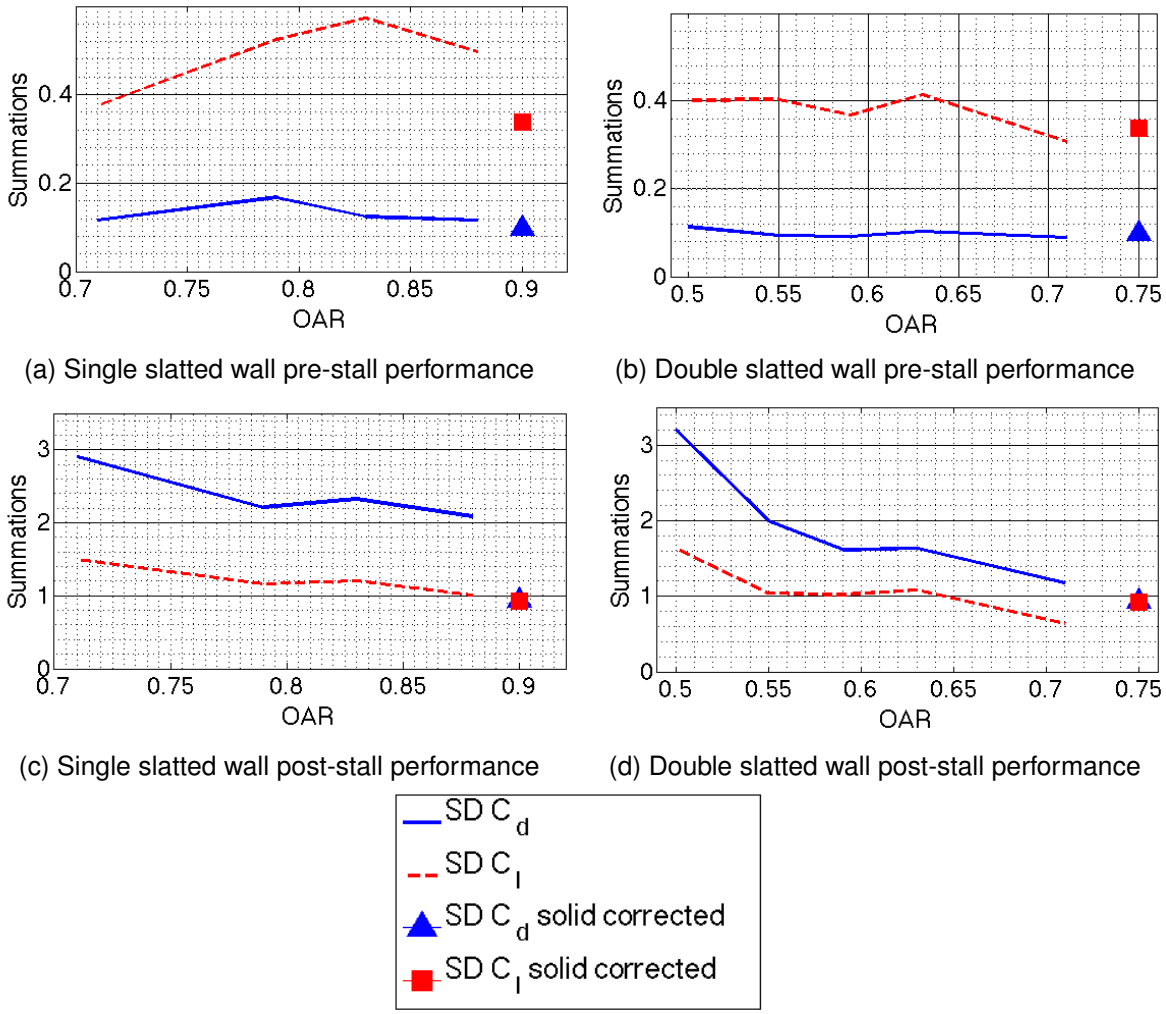

(a) Single slatted wall pre-stall performance

(b) Double slatted wall pre-stall performance

(c) Single slatted wall post-stall performance

(d) Double slatted wall post-stall performance

Figure 5: Summations of standard deviations for lift and drag, plotted against OAR. Note that while corrected solid walled data has an OAR of 0, it is shown plotted at 0.9 or 0.75.

Fig. 6 shows raw and corrected data for the solid walled tunnel, illustrating that corrections do a good job of improving data similarity across the model sizes. Fig. 7 shows results for the 71%

tolerant tunnel. Comparing the figures, it can be seen that aside from at $-75°$ to $130°$ where the tolerant tunnel over-corrects for the largest aerofoil, adversely affecting its SD score, its drag results are more consistent than those of the conventional tunnel.

Fig. 7 also includes results from the solid tunnel for the $c/H = 0.1$ aerofoil. It can be seen that results for this aerofoil, least affected by blockage and so providing the most reliable data, are consistent using either blockage reduction method.

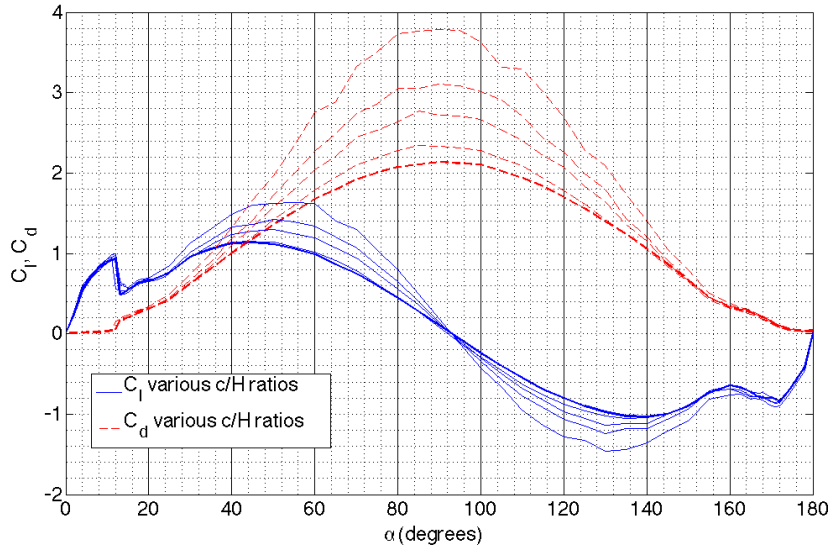

(a) Raw data

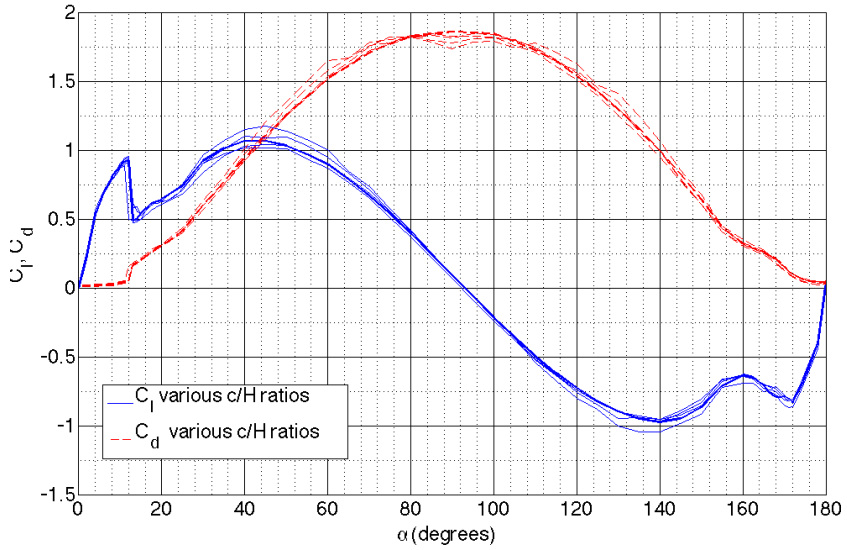

(b) Corrected data

Figure 6: C_l and C_d vs α for $c/H = 0.1, 0.15, 0.2, 0.25$ and 0.3 aerofoils taken in the solid walled tunnel. $c/H = 0.1$ results emboldened.

Using the best tunnel configuration, testing was extended to a wider range of Reynolds numbers. Fig. 8 shows the results of this work, taken using the $c/H = 0.1$ aerofoil. There is a remarkable lack of Reynolds number dependency beyond stall. Note that forces measured at $Re = 20000$

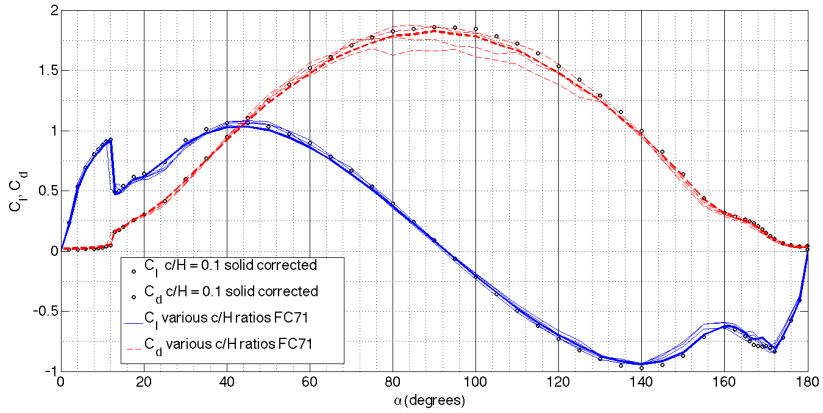

Figure 7: C_l and C_d vs α for $c/H = 0.1, 0.15, 0.2, 0.25$ and 0.3 aerofoils taken in the DS-0.71 tunnel. $c/H = 0.1$ results emboldened. Corrected solid walled data for the $c/H = 0.1$ aerofoil also included.

are approaching the resolution limits of the transducers, so results are of low accuracy. They have been included to highlight the apparent lack of any flow attachment at low incidence, an unusual phenomena.

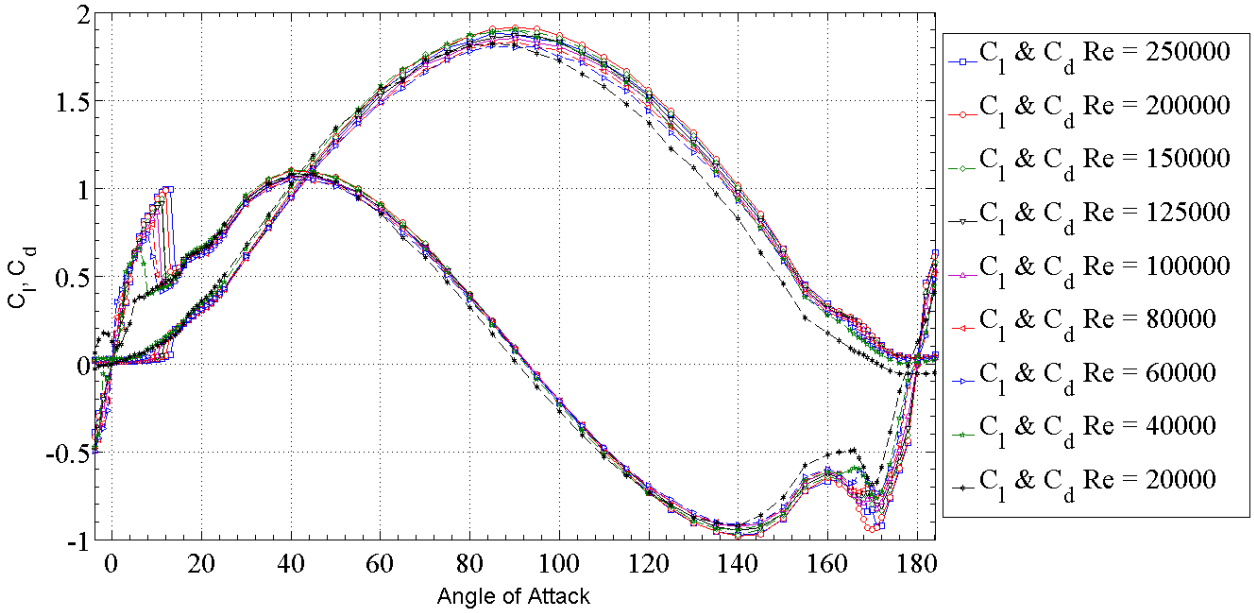

Figure 8: C_l and C_d vs α for $c/H = 0.1$ aerofoils taken in the DS-0.71 tunnel at a wide range of Reynolds numbers.

4 Conclusion

The Parkinson tolerant tunnel design, with semi-permeable walls, is shown to reduce the effects of blockage better than conventional, solid-walled tunnels using blockage corrections for aerofoils before and after stall. Since data from the tunnel can be used raw, it requires no blockage corrections

which are unsuited for use with separated flows. It therefore represents a better way of conducting post-stall aerofoil experiments to the degree of accuracy necessary for VAWT analysis.

Results for the $c/H = 0.1$ aerofoil are near identical regardless of whether using corrections or the tolerant tunnel to reduce blockage, suggesting that they are a close approximation to free air.

Results for the same aerofoil at a wide range of Reynolds numbers are presented, showing very little Reynolds number dependency beyond stall and unusual behaviour for the $Re = 20000$ case at low incidences.

5 Learning Objectives

- Demonstrate the need for better quality wind tunnel aerofoil data for the analysis of VAWTs.
- Give an overview of a rarely-used blockage-tolerant wind tunnel capable of producing such data.
- Present data from the tunnel at a range of low Reynolds numbers relevant to the analysis of domestic-scale wind turbines.

Bibliography

[1] G. Bergeles, N. Athanassiadis, and A. Michos. Aerodynamic characteristics of NACA 0012 aircraft in relation to wind generators. *Wind Engineering*, 7(4):247–262, 1983.

[2] A. Bianchini, L. Ferrari, and S. Magnani. Start-up behavior of a three-bladed H-Darrieus VAWT: experimental and numerical analysis. In *Proceedings of the ASME Turbo Expo*, pages 6–10, 2011.

[3] C.C. Critzos, H.H. Heyson, and R.W. Boswinkle. Aerodynamic characteristics of NACA 0012 airfoil section at angles of attack from 0 to 180 degrees. Technical Report TN 3361, NACA, 1955.

[4] R. Dominy, P. Lunt, A. Bickerdyke, and J. Dominy. Self-starting capability of a Darrieus turbine. *Proceedings of the Institution of Mechanical Engineers, Part A: Journal of Power and Energy*, 221(1):111–120, 2007.

[5] ESDU. Lift-interference and blockage corrections for two-dimensional subsonic flow in ventilated and closed wind-tunnels. Technical Report 76028, Engineering Sciences Data Unit, 1978.

[6] N. Hill, R. Dominy, G. Ingram, and J. Dominy. Darrieus turbines: the physics of self-starting. *Proceedings of the Institution of Mechanical Engineers Part A-Journal of Power and Energy*, 223(A1):21–29, 2009.

[7] G. Massini, E. Rossi, and S. D'Angelo. Wind tunnel measurements of aerodynamic coefficients of asymetrical airfoil sections for wind turbine blades extended to high angles of attack. In *European Community Wind Energy Conference*, pages 241–245, Herning, Denmark, June 1988.

[8] G. Parkinson. The tolerant tunnel: concept and performance. *Canadian Aeronautics and Space Journal*, 36(3):130–134, 1990.

[9] A. Pope. The forces and pressures over a NACA 0015 airfoil through 180 degrees angle of attack. Technical Report E-102, Georgia Institute of Technology, 1947.

[10] J. Rainbird. *The aerodynamic development of a vertical axis wind turbine*. MEng Project Report, University of Durham, UK, 2007.

[11] A. Rossetti and G. Pavesi. Comparison of different numerical approaches to the study of the H-Darrieus turbines start-up. *Renewable Energy*, 50(2013):7–19, 2013.

[12] R.E. Sheldahl and P.C. Klimas. Aerodynamic characteristics of seven symmetrical airfoil sections through 180-degree angle of attack for use in aerodynamic analysis of vertical axis wind turbines. Technical Report SAND80-2114, Sandia National Laboratories, 1981.

[13] J.H. Strickland. Darrieus turbine: a performance prediction model using multiple streamtubes. Technical Report SAND75-0431, Sandia National Laboratories, 1975.

[14] L.A. Viterna and R.D. Corrigan. Fixed pitch rotor performance of large horizontal axis wind turbines. In *Workshop on Large Horizontal-Axis Wind Turbines*, volume 1, pages 69–85, 1982.